Electronic Supplementary Material (ESI) for Chemical Communications

Supporting Materials

Hierarchical Cobalt Iron Oxide Nanoarrays as Structured Catalysts

Jiaqiang Sun, Yaping Li, Xijun Liu, Qiu Yang, Junfeng Liu*, Xiaoming Sun, David G. Evans and Xue Duan

Part I. Supplementary Figures and Tables

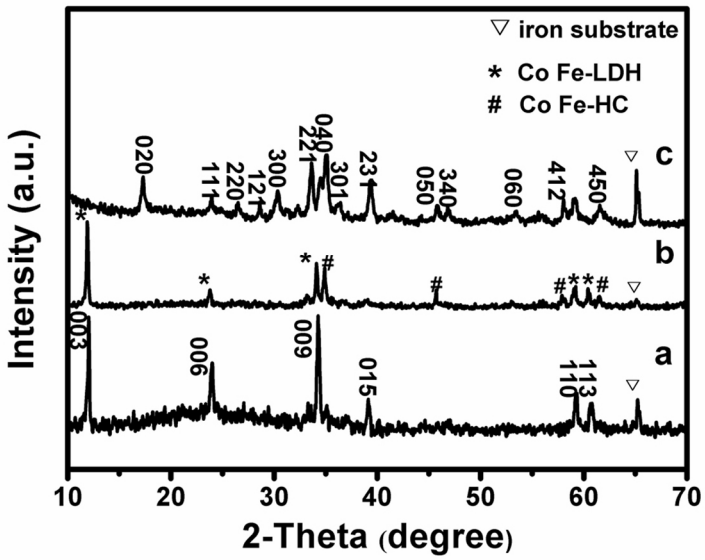

Figure S1. XRD patterns of the products formed on the iron substrate after different reaction times: (a) 3 h; (b) 4 h; (c) 12 h.

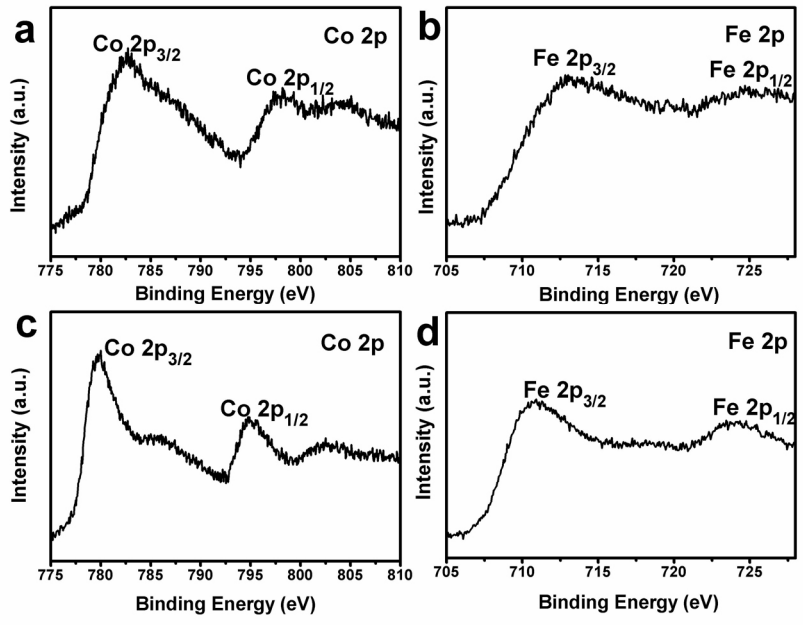

Figure S2. XPS spectra of CoFe-HC (a, b) and $Co_{3-x}Fe_xO_4$(c, d).

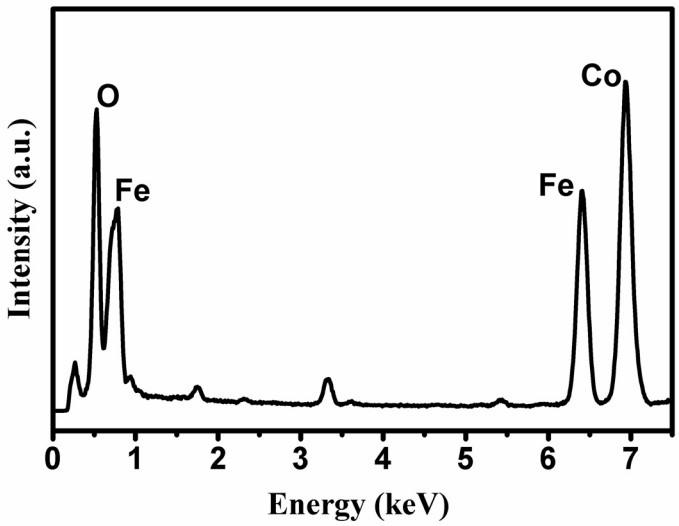

Figure S3. EDS pattern of the as-made $Co_{3-x}Fe_xO_4$ nanowire.

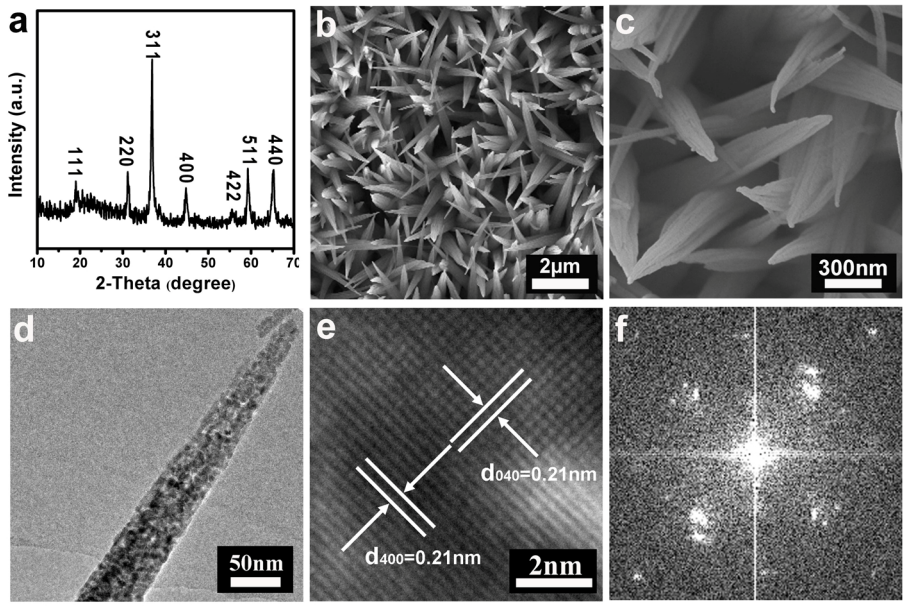

Figure S4. XRD (a), SEM (b, c), HRTEM (d, e) and FFT (f) images of Co_3O_4.

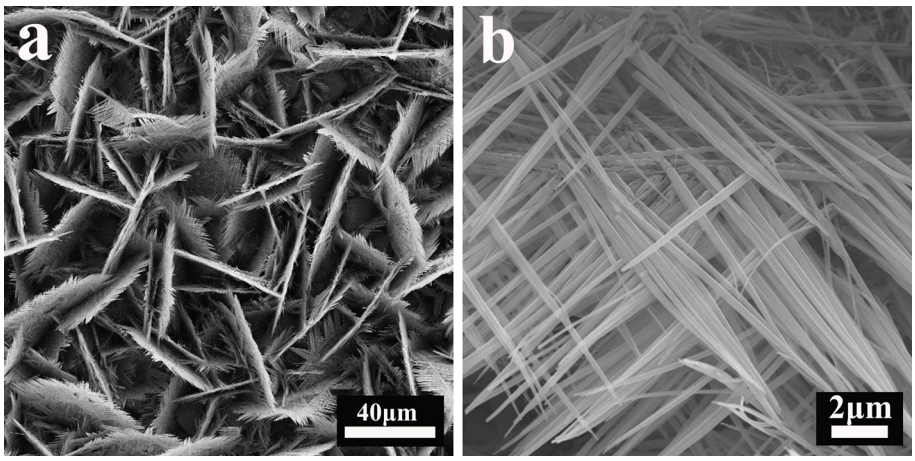

Figure S5. SEM images of $Co_{3-x}Fe_xO_4$ nanoarrays at different magnifications after being used nine times.

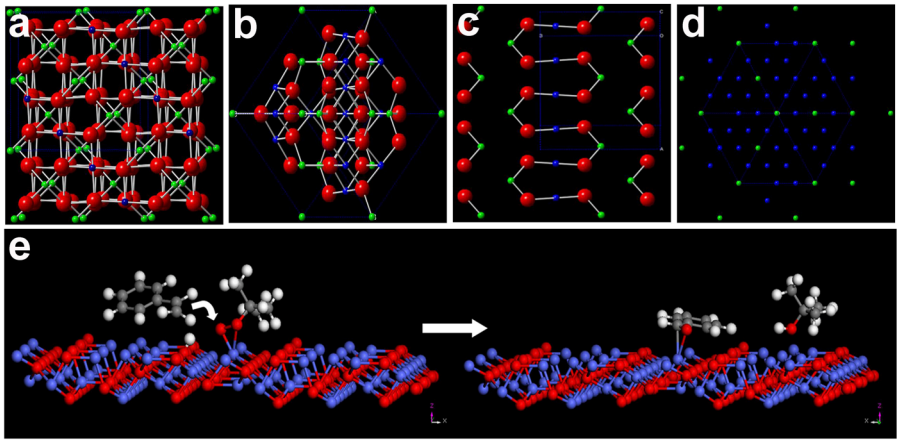

Figure S6. (a) Spinel structure of Co_3O_4; (b–d) The surface atomic configurations in the $\{1\bar{1}2\}$, $\{110\}$, and $\{1\bar{1}1\}$ planes. (e) A schematic diagram for TBHP adsorption and styrene oxidation on the active Co^{3+} sites. The red, gray, white and blue spheres are oxygen atoms, carbon atoms, hydrogen atoms and cobalt atoms, respectively.

Table S1. Electrochemical surface areas (roughness factors, Rf) of obtained materials

	CoFe-LDH	CoFe-LDH@CoFe-HC	CoFe-HC	$Co_{3-x}Fe_xO_4$
Rf	3.1	746.0	1943.1	2538

Table S2. Oxidation of styrene with TBHP catalyzed by a variety of catalysts

Catalyst	Styrene conversion (mol%)	Selectivity (mol%)		Reference
		Benzaldehyde	Styrene oxide	
$Co_{3-x}Fe_xO_4$	92.2	64.6	16.8	this study
Co_3O_4	75.1	66.5	21.4	this study
Fe_3O_4	36.0	68.0	-	1
$NiFe_2O_4$	31.4	55.6	-	1
$SrFe_2O_4$	50.8	63.7	28.0	2
$CaFe_2O_4$	38.0	91.0	-	3
$Mg_x\ Fe_{3-x}\ O_4$	32.0	63.2	-	4

Part II. Experimental Section

‡*Materials Preparation*: All chemicals were analytical grade reagents purchased from Beijing Chemical Reagents Company and used without further purification.

In a typical synthesis, 2.5 mmol of $Co(NO_3)_2{\cdot}6H_2O$, 10 mmol of NH_4F, and 12.5 mmol of $CO(NH_2)_2$ were dissolved in 50 mL of water under stirring. The homogeneous solution prepared above was transferred into a Teflon-lined stainless steel autoclave. The iron substrate was carefully cleaned with HCl (1 mol/L), absolute ethanol, and distilled water. After the cleaned iron substrate was immersed in the homogeneous solution, the autoclave was sealed and maintained at 120 ^{o}C for 12 h and then allowed to cool down to room temperature naturally. The substrate was washed several times with distilled water, dried at 80 ^{o}C for 2 h, and finally calcined in air at 400 ^{o}C for 4 h.

Co_3O_4 nanorod arrays were obtained by replacing the iron substrate with a glass slide and using a similar process to that described above.

Characterization: Powder X-ray diffraction (XRD) was performed on a Shimadzu XRD-6000 diffractometer with Cu Kα radiation (λ = 1.5418 Å) in the 2θ range from 10° to 70°. The size and morphology of as-synthesized samples were monitored by using a scanning electron microscope (SEM, Zeiss Supra 55). The structure and

composition of the products were characterized by means of a high-resolution transmission electron microscope (HRTEM, JEM 2100), energy dispersive X-ray spectroscopy (EDS) and X-ray photoelectron spectroscopy (XPS, ESCALAB 250). Samples for HRTEM were prepared by scraping the cobalt iron oxide from the substrate and ultrasonicating in ethanol, after which the suspension was dropped onto a carbon-enhanced copper grid and dried in air. The electrochemical surface areas (roughness factor) of the arrays were measured from double-layer charging curves using cyclic voltammetry.[5] The electrochemical measurements were carried out at 298 K in a three-electrode glass cell connected to an electrochemical workstation. The thin film on the iron substrate (1 cm x 1 cm) was used as a working electrode. A platinum foil (1.0 cm^2) and a saturated calomel electrode were used as a counter and reference electrode, respectively. Fresh 1 mol/L KOH aqueous solution was used as the electrolyte. The electrochemical performances of the samples were evaluated on a CHI 660D (Chen Hua, Shang Hai) workstation for cyclic voltammetry (CV).

Catalytic Reaction: Styrene oxidation was carried out in a 50 mL two-necked round bottom flask provided with a flask condenser; 1.14 mL of styrene, 1.56 mL of *tert*-butyl hydroperoxide (TBHP, 65 wt.%) 10 mL of acetonitrile and the $Co_{3-x}Fe_xO_4$ nanoarray catalyst (about 0.1 g of $Co_{3-x}Fe_xO_4$) were added successively to the flask under stirring. Then the mixture was heated to 80 ^oC in an oil bath for 12 h. The oxidation process was repeated nine times using the same catalyst. The catalytic reaction was monitored by carefully withdrawing small amounts of the reaction liquid with a microsyringe from the flask. The products were identified and quantified using a gas chromatograph (GC-SP-6890, SE-30 capillary column, 30 m × 0.32 mm) with a flame ionization detector, nitrogen as carrier gas and a constant oven temperature (120 ^oC). Both the injector and detector temperature were 300 ^oC. The reactant conversion and product (i) selectivity were calculated as follows:

$$\text{styrene conversion (mol\%)} = \frac{\text{moles of reactant converted}}{\text{moles of reactant in feed}} \times 100 \quad (1)$$

$$\text{product (i) selectivity (mol\%)} = \frac{\text{moles of product (i)}}{\text{moles of reactant converted}} \times 100 \quad (2)$$

Part III. Theoretical calculations using the DFT method for different surface

As shown in Figure S6a, Co_3O_4 has a spinel structure, in which oxygen anions form a distorted fcc sublatttice, Co^{3+} cations occupy half of the octahedral interstices and Co^{2+} cations occupy one-eighth of the tetrahedral interstices. The Co^{3+} ions are regarded as the active site for oxidation, whereas the Co^{2+} ions are almost inactive.[6, 7, 8]

The density functional theory (DFT)–ONIOM method was used to calculate all geometry optimizations with the Gaussian 09 program package.[9] The lower energy structures were obtained using the two-layer ONIOM methodology as shown below. A universal force field (UFF) approach was employed for the Low level, while for High level, the calculations were performed using the DFT approach (B3LYP), with the 6-31G basis set for C, H, and O atoms and the effective core potential (ECP) of the LANL2DZ basis set for Co, Fe atoms.[10, 11.]

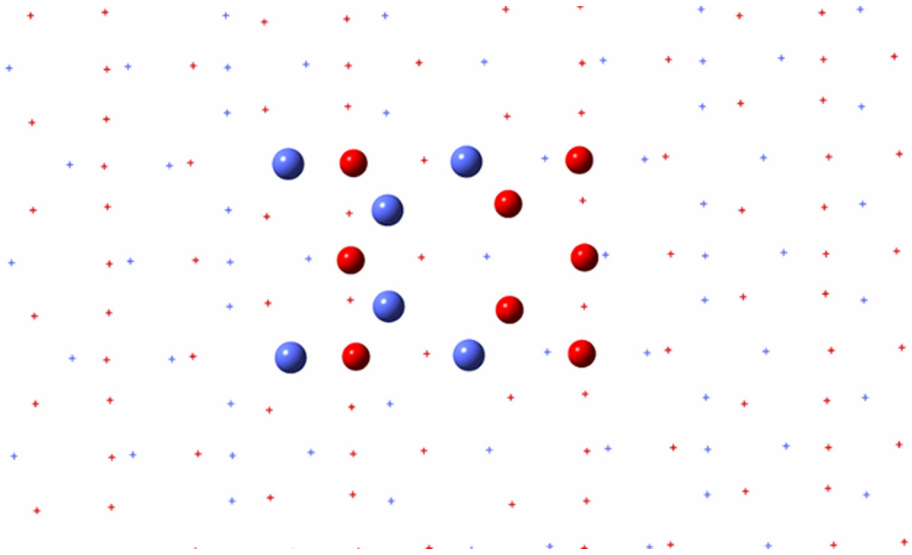

The Co_3O_4 (112) model.

High level: ball and stick. Low level: wireframe. Blue: Co. Red: O.

The adsorption energy for TBHP is –312 kJ/mol on the $(1\bar{1}2)$ surface and –297 kJ/mol on the (110) surface, whilst for styrene it is –169 kJ/mol on the $(1\bar{1}2)$ surface and –125 kJ/mol on the (110) surface, indicating $\{1\bar{1}2\}$ planes are more active than other surfaces in the styrene catalytic oxidation. Therefore, it is most likely that

styrene oxidation on the $Co_{3-x}Fe_xO_4$ nanowires follows the reaction pathway shown in Figure S6e. Firstly, the TBHP molecule adsorbs preferably on the surface Co^{3+} cation to form reactive molecular oxygen. Secondly, the oxidation of styrene then occurs by abstracting the surface reactive oxygen coordinated with Co^{3+} cations.

References:

1 D. Guin, B. Baruwati, S. V. Manorama, *J. Mol. Catal. A: Chem.* 2005, **242**, 26.

2 S. K. Pardeshi, R. Y. Pawar, *J. Mol. Catal. A: Chem.* 2011, **334**, 35.

3 S. K. Pardeshi, R. Y. Pawar, *Mater. Res. Bull.* 2010, **45**, 609.

4 N. Ma, Y. Yue, W. Hua, Z. Gao, *Appl. Catal. A: Gen.* 2003, **251**, 39.

5 J.O'M. Bockris, T. Otagawa, *J. Electrochem. Soc.* 1984, **131**, 290.

6 X. Xie, Y. Li, Z.-Q. Liu, M. Haruta, W. Shen, Nature 2009, **458**, 746.

7 K. Omata, T. Takada, S. Kasahara, M. Yamada, *Appl. Catal. A: Gen.* 1996, **146**, 255.

8 J. P. Jacobs, A. Maltha, J. G. H. Reintjes, J. Drimal, V. Ponec, H. H. Brongersma, *J. Catal.* 1994, **147**, 294.

9 Gaussian 09, Revision B.01, M. J. Frisch, G. W. Trucks, H. B. Schlegel, G. E. Scuseria, M. A. Robb, J. R. Cheeseman, G. Scalmani, V. Barone, B. Mennucci, G. A. Petersson, H. Nakatsuji, M. Caricato, X. Li, H. P. Hratchian, A. F. Izmaylov, J. Bloino, G. Zheng, J. L. Sonnenberg, M. Hada, M. Ehara, K. Toyota, R. Fukuda, J. Hasegawa, M. Ishida, T. Nakajima, Y. Honda, O. Kitao, H. Nakai, T. Vreven, J. A. Montgomery, Jr., J. E. Peralta, F. Ogliaro, M. Bearpark, J. J. Heyd, E. Brothers, K. N. Kudin, V. N. Staroverov, T. Keith, R. Kobayashi, J. Normand, K. Raghavachari, A. Rendell, J. C. Burant, S. S. Iyengar, J. Tomasi, M. Cossi, N. Rega, J. M. Millam, M. Klene, J. E. Knox, J. B. Cross, V. Bakken, C. Adamo, J. Jaramillo, R. Gomperts, R. E. Stratmann, O. Yazyev, A. J. Austin, R. Cammi, C. Pomelli, J. W. Ochterski, R. L. Martin, K. Morokuma, V. G. Zakrzewski, G. A. Voth, P. Salvador, J. J. Dannenberg, S. Dapprich, A. D. Daniels, O. Farkas, J. B. Foresman, J. V. Ortiz, J. Cioslowski, and D. J. Fox, Gaussian, Inc., Wallingford CT, 2010.

10 A. D. Becke, *Phys. Rev. A* 1988, **38**, 3098.

11 C. Lee, W. Yang, R. G. Parr, *Phys. Rev. B* 1988, **37**, 785.